Agricultural Water Management 177 (2016) 54–65

Contents lists available at ScienceDirect

Agricultural Water Management

journal homepage: www.elsevier.com/locate/agwat

Optimizing drip irrigation for eggplant crops in semi-arid zones using evolving thresholds

T. Müller[a,b,*], C. Ranquet Bouleau[a], P. Perona[b,c]

[a] Cooperation & Development Center (CODEV), Ecole Polytechnique Fédérale de Lausanne (EPFL), Lausanne, Switzerland
[b] Laboratory of Applied Hydroeconomics and Alpine Environmental Dynamics (AHEAD), Ecole Polytechnique Fédérale de Lausanne (EPFL), Lausanne, Switzerland
[c] Institute for Infrastructure & Environment, School of Engineering, The University of Edinburgh, UK

ARTICLE INFO

Article history:
Received 26 November 2015
Received in revised form 1 June 2016
Accepted 20 June 2016
Available online 9 July 2016

Keywords:
Triggered drip irrigation
Soil matric potential threshold
Eggplant
Irrigation water management
Soil water modeling
Semi-arid regions

ABSTRACT

Field experiments were combined with a numerical model to optimize drip irrigation management based on soil matric potential (SMP) measurements. An experimental crop of eggplant was grown in Burkina Faso from December 2014 to March 2015 and plant response to water stress was investigated by applying four different irrigation treatments. Treatments consisted in using two different irrigation depths (low or high), combined with a water provision of 150%, 100% or 66% (150/100/66) of the maximum crop evapotranspiration (T150low, T66low, T100high, T66high). Soil matric potential measurements at 5, 10 and 15 cm depth were taken using a wireless sensor network and were compared with measurements of plant and root biomass and crop yields. Field data were used to calibrate a numerical model to simulate triggered drip irrigation. Different simulations were built using the software HYDRUS 2D/3D to analyze the impact of the irrigation depth and frequency, the irrigation threshold and the soil texture on plant transpiration and water losses. Numerical results highlighted the great impact of the root distribution on the soil water dynamics and the importance of the sensor location to define thresholds. A fixed optimal sensor depth of 10 cm was found to manage irrigation from the vegetative state to the end of fruit development. Thresholds were defined to minimize water losses while allowing a sufficient soil water availability for optimal crop production. A threshold at 10 cm depth of −15 kPa is recommended for the early growth stage and −40 kPa during the fruit formation and maturation phase. Simulations showed that those thresholds resulted in optimal transpiration regardless of the soil texture so that this management system can constitute the basis of an irrigation schedule for eggplant crops and possibly other vegetable crops in semi-arid regions.

1. Introduction

Semi-arid regions in sub-Saharan Africa rely on irrigation for agricultural activities during the dry season, characterized by extreme temperature and dry wind conditions, and an almost total absence of precipitation. Agriculture traditionally takes place during the rainy season, but the impacts of climate change, the shift of rainfalls to the South, the great variability of interannual rainfall and the severity of drought pockets have made dry season agriculture crucial for food security (FAO, 2014).

Water is a scarce resource in semi-arid regions, and high yields are difficult to obtain. FAO (2014) estimates that, in 2014, 80% of the food was produced by family farmers in a sample of 30 countries and further states that they must innovate to tackle a triple challenge: yield growth to meet the world's needs for food security and better nutrition; environmental sustainability to protect soil and water resources in relation to their own productive capacity; productivity growth and livelihood diversification to lift themselves out of poverty and hunger.

While technologies such as drip irrigation kits reduce the time spent to irrigate the crop and improve water allocation by only irrigating near the root zone, estimating adequate water needs and timing to maximize yields remains a challenge. Irrigation is usually done on a visual assessment of the soil and plant state, and producers mostly rely on their own experience, often resulting in over-irrigation and water losses. In this context, the recent development of autonomous wireless sensor networks offers new perspectives for precise triggered irrigation (Barrenetxea et al., 2008; Ranquet Bouleau et al., 2015).

* Corresponding author at: Cooperation & Development Center (CODEV), Ecole Polytechnique Fédérale de Lausanne (EPFL), Lausanne, Switzerland.
E-mail address: tom.muller1@gmail.com (T. Müller).

http://dx.doi.org/10.1016/j.agwat.2016.06.019

An appropriate irrigation schedule aims at avoiding plant water stress by optimizing the soil water availability in the root zone. Water stress first modifies the plant's turgor pressure and affects cell growth and wall synthesis (Laio et al., 2001) which is particularly problematic during the plant's vegetative and development stages. During the plant's mid-season and yield formation, water stress can be identified by stomatal closure leading to reduced transpiration followed by pollination failure (Steduto et al., 2012). In FAO's models (Raes et al., 2012), a parameter *p*, which characterizes the fraction of soil water depletion in the whole root zone, is used to determine the degree of water stress and its impact on yield. This parameter is difficult to assess on-site, and other methods to manage irrigation have therefore been investigated. Other parameters to track water stress are based either on direct monitoring of the plant response (tissue water potential, Thompson et al., 2007, or sap flow, Patakas et al., 2005), on plant remote sensing (infrared thermometry, Taghvaeian et al., 2012) or indirectly by measuring the soil water availability (soil water content or soil matric potential).

Managing irrigation using soil matric potential (SMP) thresholds has shown a promising potential for saving water and improving yields with the use of simple sensors. In contrast to soil water content monitoring, SMP thresholds are less dependent on the soil texture since the SMP is directly linked to the plant's root ability to uptake water. An important challenge of SMP based irrigation is that measurements are done at specific locations which may not be representative of the SMP in the whole root zone, as root water uptake depends on root density. Table 1 lists selected recent scientific articles proposing thresholds to trigger irrigation given the crop type. It can be observed that no clear consensus seems to emerge from those studies as experiment-specific conditions lead to great differences in optimal thresholds, even with a relatively similar soil texture or crop type. Comparisons are especially difficult as the sensor is placed at different depths in a soil profile where water availability is not homogeneous. Most studies also propose thresholds only for the mid-season when transpiration is maximal, but do not consider previous growth stages where water losses due to evaporation are greater and important water savings may be achieved.

In this context, the research project Info4Dourou2.0 based at the Ecole Polytechnique Fédérale de Lausanne (EPFL) has developed an innovative autonomous wireless sensor network based on continuous SMP measurements that is adapted to extreme climates (Ranquet Bouleau et al., 2015). Relying on this wireless sensor network, the main objective of this study was to set the basis for an optimized irrigation management system using SMP measurements that can be more easily reproduced, compared and that can provide simple and practical recommendations for local producers or engineers. The system is primarily designed for family farmers in semi-arid regions, and the goal was to use a single SMP sensor at a certain depth to make it more affordable.

We first focused on the plant response to water stress during the whole plant growth and the impact of the irrigation schedule on aerial biomass and root development. In a second phase, a numerical model was built using the software HYDRUS 2D/3D in order to achieve a more comprehensive understanding of the spatial soil water distribution and to optimize the sensor placement and irrigation thresholds. Dabach et al. (2013) showed the potential of the software to simulate the evolution of the SMP and to optimize the irrigation threshold, but only tested high threshold values (−3 to −20 kPa). In this paper, simulations were created to assess the impact of different irrigation depths and frequencies and thresholds on the water fluxes (evaporation, transpiration, leakages). The final outcomes of the paper were: (i) to select an optimized sensor location; (ii) to define appropriate irrigation thresholds for each eggplant growth stages; (iii) to assess the influence of the soil texture on the proposed management system.

2. Materials and methods

2.1. Experimental site

The experiments were conducted in a rural area 8 km away from Ouagadougou, Burkina Faso (12°20′24″ N, 1° 27′8″ O). The experiments took place from December 5, 2014 to March 25, 2015 on a drip irrigation system of 200 m^2 cultivated with eggplants. The species of eggplant selected was *Kalenda*. Before transplanting, the soil was ploughed manually to a depth of 10 cm. 1 kg/m^2 of a NPK soil amendment and 0.25 kg/50 m^2 of urea were also applied homogeneously over the crop before transplantation. The drip irrigation kits were provided by the non-profit social enterprise "International Development Enterprises" (iDE). The 200 m^2 drip irrigation system consisted of 24 sublines, 8 m long, separated by 1 m between rows. Each subline was equipped with 15 drippers with a spacing of 0.5 m. Drippers consisted of small microtubes with a discharge rate of about 2.5 l/h. The irrigation water was pumped from a dam 250 m away and stored in a 1 m^3 reservoir. One eggplant was transplanted at about 2 cm from each microtube. The soil texture corresponded to a compact sandy clay loam soil, with very poor organic matter. A hard layer of ferralitic rock, made of partially crumbly rock mixed with some sandy earth, was located at a depth of 25–30 cm.

2.2. Irrigation treatments

The parcel was divided into four subplots consisting of 6 sublines each. 90 eggplants were planted on each subplot, they had a total canopy cover of 17.7 m^2 at full growth. The irrigation depth was calculated by dividing the total water volume applied to the subplot in liters by the total wetted area of the drippers in square meters. The wetted radius of each dripper was estimated to 0.25 m which corresponded to the radius of the canopy at full growth. The four irrigation treatments were coded as T150low, T66low, T100high and T66high. The code number (150/100/66) corresponds to the percentage of water needs that were provided for each treatment. Water needs in mm/day were established based on standard crop evapotranspiration (ET_c) given the crop growth stage. The code "low" or "high", identifies the type of schedule. For "low" treatments, a fixed water amount of 5.6 mm (l/m^2) was applied to each irrigation event, and the irrigation frequency was defined to meet the corresponding percentage of ET_c. 5.6 mm corresponded to the standard depth applied by the local producers and was considered low as it represented only 35% of the readily available water (RAW) (Allen et al., 1998). "High" treatments received a higher irrigation depth corresponding to 150% of the RAW, which was adapted for each growth stage because of root growth. This led to a lower irrigation frequency to meet the corresponding water needs. A fixed irrigation schedule was defined for each treatment and for each growth stage, summarized in Table 2.

T150low is the control experiment and follows the practice of local producers. The "low" irrigation depth corresponded to 5.6 mm and irrigation was triggered twice a day as done by producers. This practice corresponded to providing 150% of the estimated ET_c during the mid-season. For T66low, the same "low" irrigation amount was applied but only 66% of the ET_c was restored by using a lower irrigation frequency than T150low, so that water stress was induced. T100high received a "high" irrigation depth and a lower irrigation frequency to meet 100% of ET_c. Finally, T66high received the same "high" irrigation amount but only 66% of ET_c was provided. The different treatments began 20 days after

Table 1
Literature review of proposed SMP irrigation thresholds for different crops in the last decade.

Author	Crop type	Threshold [kPa]	Sensor depth [cm]	Growth stage	Soil type
Oliveira et al. (2011)	Cucumber	−30	12.5	Crop development	Dystroferric red latosol
Oliveira et al. (2011)	Cucumber	−15	12.5	Mid-season	Dystroferric red latosol
Bilibio et al. (2010)	Eggplant	−15	12.5	Mid-season	?
Thompson et al. (2007)	Melon	−35	10	Mid-season	Sandy loam
Enciso et al. (2009)	Onion	−30	20	Mid-season	Sandy clay loam
Thompson et al. (2007)	Pepper	−58	10	Mid-season	Sandy loam
Coolong et al. (2012)	Pepper	−60	20	Mid-season	Silt loam
Liu et al. (2012)	Chili-Pepper	−30 to −40	20	Mid-season	Sandy loam
Wang et al. (2007b)	Potato	−25 to −35	20	Mid-season	Loam
Kang and Wan (2005)	Radish	−35 to −55	20	Mid-season	Silt loam
Wang et al. (2007a)	Tomato	−50	20	Mid-season	Silt loam
Coolong et al. (2011)	Tomato	−45	20	Mid-season	Silt loam
Zheng et al. (2013)	Tomato	−40	25	Mid-season	Silt
Marouelli and Silva (2007)	Tomato	−35	10	Crop development	Clayey oxysol
Marouelli and Silva (2007)	Tomato	−12	15	Mid-season	Clayey oxysol
Marouelli and Silva (2007)	Tomato	−15	20	Maturation	Clayey oxysol
Wang et al. (2005)	Tomato	−30	?	Mid-season	Gravelly loam
Thompson et al. (2007)	Tomato	−38 to −58	10	Mid-season	Sandy loam

Table 2
Irrigation schedules used for the four treatments on the eggplant crop. The different growth stages used by the FAO (Allen et al., 1998) and their corresponding length defined as days after transplanting (DAT) are also shown.

Growth stage	DAT	T150low		T66low		T100high		T66high	
[–]	[days]	Frequency [1/day]	Depth [mm]	Frequency [1/day]	Depth [mm]	Frequency [1/day]	Depth [mm]	Frequency [1/day]	Depth [mm]
Initial growth	0–20	2	5.6	1/1	5.6	1/1	5.6	1/1	5.6
Crop development	20–60	2	5.6	1/1.5	5.6	1/2	11.3	1/3	11.3
Mid-season	60–100	2	5.6	1/1.25	5.6	1/3	22.6	1/4	22.6
Late season	100–120	2	5.6	1/1.5	5.6	1/4	22.6	1/5	22.6

transplanting (DAT), when the plants were well established. Those four treatments allowed us to assess both the impact of the irrigation schedule (irrigation depth and frequency) and the effect of water stress (percentage of ET_c provided).

2.3. Crop evapotranspiration and readily available water

The reference evapotranspiration (ET_0) was calculated according to the directive from the FAO, using the original Penman–Monteith equation (Allen et al., 1998). Air temperature, relative humidity and solar radiation were obtained using a Decagon VP-3 sensor for temperature and humidity and a Davis Solar Radiation sensor, which were connected to an automatic meteorological station located in the center of Ouagadougou, 8.4 km away from the experimental site. Wind measurements and precipitation amounts were taken on site for more precision with a Davis Anemometer and a Davis Rain Collector. The time resolution of the data was 1 min and data were accessible in real time on a web interface. ET_0 calculations were validated by comparison with historical data from the FAO and the National Meteorological Institute of Burkina Faso. Crop maximal evaporation (ET_e) and transpiration (ET_{cb}) were distinguished from the crop evapotranspiration (ET_c) by using the dual crop coefficients (k_e and k_{cb}) (Allen et al., 1998). The dual crop coefficients suggested by the FAO were used and were adapted to the wind speed and relative humidity as suggested in Allen et al. (1998).

The readily available water (*RAW*) was calculated by estimating the soil moisture at field capacity (θ_{fc}) and permanent wilting point (θ_{pwp}), using the average fraction of total available soil water that can be depleted from the root zone (p) suggested by the FAO in Allen et al. (1998) and using direct measurements of the maximum rooting depth. Table 3 summarizes climatic and plant data for the different growth stages.

2.4. Soil measurements

The SMP was monitored every minute using Watermark sensors from Irrometer which were connected to an autonomous wireless sensor network and data were accessible in real-time on a web interface. For each treatment, the SMP was measured on 2 plants, at 5, 10 and 15 cm depth. In one case, the sensors were placed at a horizontal distance of 5 cm from the dripper, while on the second plant, the distance was 12 cm. Additionally, two soil moisture sensors, a 5TE and a 5TM from Decagon, were placed close to a Watermark sensor at 10 cm depth to compare both measurements and to draw the relationship between soil moisture and SMP.

2.5. Plant measurements

Plant growth was monitored weekly during the whole growth, starting 20 days after transplanting. Measurements included (i) the diameter of the stem, 2 cm above ground; (ii) the mean diameter of the canopy cover of each eggplant; (iii) the plant height; (iv) the total number of leaves; (v) the number of flowers and (vi) the weight of harvested fruits. For each treatment, measurements were collected on a sample of 10 eggplants selected randomly among a total amount of 90.

Table 3
Estimated climatic parameters. K_c is the single crop coefficient; ET_0 is the reference evapotranspiration; z_r is the root depth; p is the total available soil water that can be depleted from the root zone and *RAW* is the readily available water. Based on Allen et al. (1998).

	K_c [–]	ET_0 [mm/day]	z_r [m]	p [-]	*RAW* [mm]
Initial growth	0.6	5.23	0.1–0.2	0.45	3.6–7.2
Crop development	0.6-1.1	5.76	0.2–0.4	0.45	7.2–14.4
Mid-season	1.1	6.63	0.4	0.45	14.4
Late season	1.04	5.81	0.4	0.45	14.4

Table 4
Soil model parameters. θ_r is the residual water content; θ_{pwp} is the water content at permanent wilting point; θ_{fc} is the water content at field capacity; θ_s is the saturated water content; α and n are calibration parameters and K_s is the saturated hydraulic conductivity.

θ_r [cm^3 cm^{-3}]	θ_{pwp} [cm^3 cm^{-3}]	θ_{fc} [cm^3 cm^{-3}]	θ_s [cm^3 cm^{-3}]	α [cm^{-1}]	n [–]	K_s [cm/day]
0.102	0.1054	0.1858	0.315	0.0558	1.6328	15

The root structure was analyzed by directly extracting the root system from the soil. The ground around the plant was excavated and a large volume of soil containing the majority of roots was extracted. The earth and rocks were then washed away. Samplings were done on two plants for each treatment at 30, 55 and 75 days after transplanting. The one dimensional root distribution was assessed by image processing. A picture of the root distribution was taken, processed into a black and white image and the density with depth was measured by summing up the number of black pixels for each layer as also done by Pasquale et al. (2012). Statistical validation of root distribution differences between treatments was not possible as only one to two root extractions occurred for each treatment.

2.6. Numerical model

HYDRUS 2D/3D (Šimůnek et al., 2012) is a dedicated software that simulates water, heat and solute movements in two dimensional unsaturated soils. It allows you to simulate soil evaporation, transpiration and root water uptake, as well as water stress. The 2.04 2D-lite version of the numerical model was used to test different irrigation schedules and irrigation thresholds, and to assess the degree of water stress and the irrigation amounts. The simulation domain consisted of a simple 2D vertical rectangular domain. The discretization of the domain had a grid spacing of 10 mm for the z-coordinate and 25 mm for the *x*-coordinate. The boundary conditions were "Atmospheric Boundary conditions" for the top soil evaporation rate, "Variable Flux 1" for the dripper fluxes and "Free Drainage" at the bottom.

The parameters for the soil hydraulic properties were based on the van Genuchten–Mualem equations (Genuchten, 1980). A soil water retention curve (SWRC) was drawn with the field data which allowed the calibration of the unknown parameters by minimizing the Root Mean Square Error (RMSE) between the modeled and measured SWRC. The calibration matched the characteristics of a Sandy Clay Loam texture proposed in HYDRUS 2D/3D and a similar parameterization was done by Mermoud et al. (2005) in an experimental field 17 km away from our site. The parameters used for the model are summarized in Table 4. For calibration only, a reduced saturated hydraulic conductivity of 5 cm/day was used at a depth of 300 mm to simulate the rocky soil layer.

The root water uptake stress function responsible for transpiration reduction was based on the model proposed by Genuchten (1987). The following values were calibrated with field measurements: h_{50} = −50 kPa and p = 3 which allows an early decrease in transpiration (50% uptake reduction at −50 kPa (h_{50}); 18% at −30 kPa; 6% at −20 kPa). The same calibration was also used by Dabach et al. (2015) for an eggplant crop. HYDRUS 2D/3D also implements a dimensionless water stress index ω_c (Šimůnek and Hopmans, 2009), which allows you to compensate for the root water uptake reduction in a certain zone by increasing the water uptake in other parts of the root zone. Compensation therefore allows the sustainment of maximal transpiration even when a small part of the root zone is stressed. ω_c has a value between 0 (full compensation) and 1 (no compensation). Deb et al. (2011) showed that compensation (ω_c<0.5) significantly improves the simulation of the water uptake from deep layers and Yadav et al. (2009) confirmed that it plays an important role in maintaining the transpiration rate when water stress occurs in the top soil layers. After calibration, a ω_c value of 0.7 was selected for our simulations. The spatial distribution of the root water uptake was defined in 2D, based on direct measurements of the extracted root systems.

2.7. Triggered irrigation scenarios

Scenarios were built to assess the effect of different irrigation depths and thresholds on water stress and water consumption. We used, for all scenarios, similar soil calibration, similar water stress function and the same simulation duration, as well as the same evaporation and transpiration rates. In HYDRUS 2D/3D, irrigation can be triggered by specifying an observation node which corresponds to the sensor location. When the SMP falls below a defined value at that node, an irrigation event is triggered with a specific irrigation time and rate. HYDRUS 2D/3D does not implement a time lapse between irrigation events that is different from the irrigation time. Consequently, if the wetted front of an irrigation event does not reach the desired sensor depth within the irrigation time, a second irrigation event is triggered, doubling the irrigation depth. This precluded modeling triggered irrigation at lower sensor depths than 5 cm for scenarios with low irrigation depth up to 5.6 mm.

Two different growth periods were analyzed. The first period corresponded to the initial growth stage, between days 10 and 30 after transplanting. The second period corresponded to the mid-season, during yield formation, between 80 and 100 days after transplanting. For the first period, the thresholds tested were: −5, −10, −15, −20, −25, −30, −35, −40, −50 and −100 kPa. These scenarios were also tested with different irrigation depths corresponding to 1.4 mm (38% RAW), 2.8 mm (75% RAW) and 5.6 mm (150% RAW). For the mid-season period, the thresholds were: −5, −10, −20, −30, −40, −50, −70, −100, −150 and −200 kPa. The different irrigation depths corresponded to 5.6 mm (38% RAW), 11.3 mm (75% RAW) and 22.6 mm (150% RAW). For scenarios with an irrigation lower than or equal to 5.6 mm, the threshold was located at a depth of 5 cm and 5 cm away from the dripper horizontally. For higher irrigation depths, a threshold at 10 cm depth was also considered.

3. Results

3.1. Soil matric potential and plant growth

Continuous measurements of the SMP and plant growth were collected from days 20–100 after transplanting for the sensors at 5 and 15 cm depth, 12 cm away from the microtubes (Fig. 1).

In Fig. 1, due to the day-to-day variability of the weather conditions, water needs and the fixed irrigation schedule, the SMP does not show a completely cyclic behavior, so that irrigation does not occur for the same value of SMP. The sensors at two different depths illustrate that the SMP in the root zone is not constant with depth. Treatment T150low keeps SMP values close to 0 kPa because of the frequent irrigation events and the provision of 150% of the water needs. For treatment T66low, the sensor at 15 cm depth becomes disconnected from the wetted bulb due to the small irrigation amounts and its value drops rapidly below −200 kPa. T100high

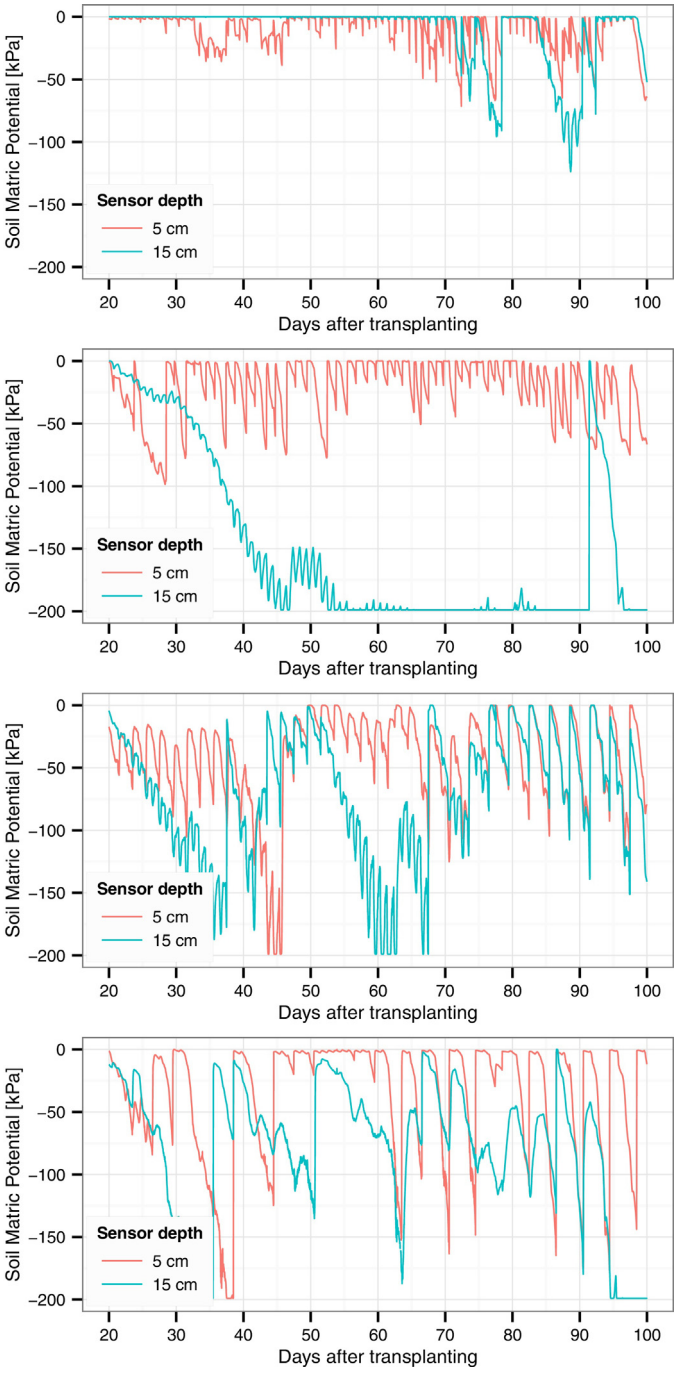

Fig. 1. Evolution of the soil matric potential for T150low, T66low, T100high, T66high (top to bottom) for sensors at 5 and 15 cm depth, 12 cm away from a microtube.

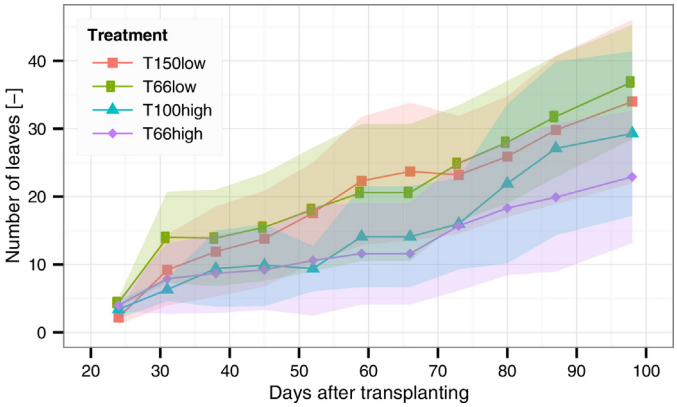

Fig. 2. Evolution of the number of leaves for all treatments. Lines show the mean values while ribbons represent 1 standard deviation.

and T66high show lower SMP values due to the lower irrigation frequency, but the soil is recharged more in depth than T66low due to the higher irrigation depth. On 45 DAT, a very short rainy event (0.5 mm) occurred, leading to lower root water uptake and an increase in SMP during the next irrigation event.

The evolution of plant growth is illustrated in Fig. 2. Only the total number of leaves is shown as an example, since there was a high correlation between the different measurements ($r > 0.8$) and statistical analyses were similar.

The Student's t-test was used to determine if samples of plant growth for each treatment were significantly different in Fig. 2. The normality of the samples was confirmed using a ShapiroWilk test, and samples were considered different when the p-value of the t-test was lower than 0.05 ($p < 0.05$). The results indicate that plants from T100high and T66high became significantly different from T150low and T66low starting 52 days after transplanting (p-value between 0.003 and 0.037). T66high remains different until the end of the experiment, while T100high was no longer significantly different after 80 DAT.

A "non-identified" vascular disease, which attacked the roots and led to ripening of the plant, infected the crop at the beginning of the flowering period, 60 DAT, and was particularly severe in T150low and T100high. The sensors were only placed on healthy plants, so that the disease did not affect the measurements of the SMP. At the end of the experiment the following percentages of plants were left: 18.6% for T150low, 84.9% for T66low, 41.8% for T100high and 83.7% for T66high. In order to analyze the effect of water stress on plant growth, only the area of healthy plants, which growth was mainly influenced by the SMP, was considered. This procedure was acceptable since it was observed that the disease was not directly linked to high soil moisture. Indeed, from Fig. 1, the SMP of T100high reaches values below −50 kPa every 2–3 days, while T66low presented much higher SMP values at 5 cm but suffered from the least plant losses. From this observation and the spatial diffusion of the disease, it seems that the disease was randomly spread in all experiments at first. T150low and T100high favored the diffusion of the disease to neighboring plants, as those treatments allowed a wider soil moisture recharge between two plants after an irrigation event. As a result, the disease was instead linked to the spatial distance between plants and the connection of wetted bulbs.

Table 5 shows the total harvest of each treatments. The relative yields were calculated by dividing the harvest weight by the crop area of healthy plants. The irrigation water use efficiency (IWUE) was calculated by dividing the relative yield by the total amount of irrigation water applied and multiplied by the total crop area. Reported mean yields for eggplants in Burkina Faso and Ivory Coast are around 20 T/ha (2 kg/m^2) (Fondio et al., 2009; Anon, 2003).

Table 5
Marketable harvests for the eggplant experiment.

	Harvest [kg]	Relative yield [kg/m^2]	IWUE [kg/m^3]
T150low	10.5	2.12	1.664
T66low	23.7	1.09	1.894
T100high	10.3	0.97	1.221
T66high	9.7	0.44	0.690

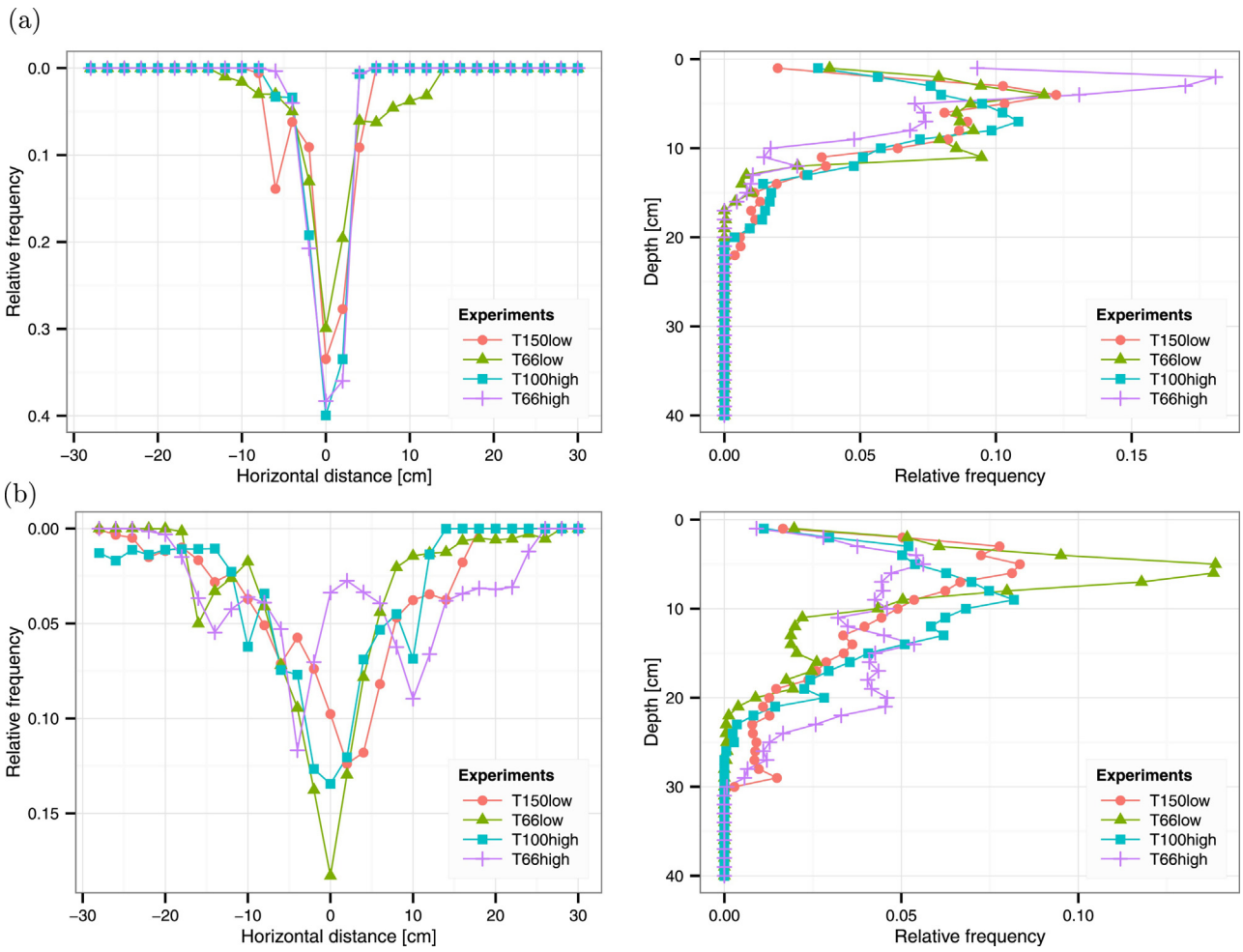

Fig. 3. Horizontal and vertical root density for all treatments at (a) 30 DAT and (b) 55 DAT.

3.2. Root development

Fig. 3 shows the root density measured both horizontally away from a dripper and vertically with depth, at 30 and 55 DAT. No significant root density changes occurred between 55 and 75 DAT. At each growth stage, the general pattern of root length density for all extractions was similar, regardless of treatment. Density increases sharply from the ground to a depth of between 5 and 12.5 cm, with a mean at 7 cm depth and then decreases relatively linearly to the maximal root depth. For the horizontal distance, a relatively linear decrease in root water uptake until the maximal length was observed. Such a profile was similar to other studies Coelho and Or (1998) and well reflects the water availability in the field. Differences between treatments due to water stress are not clear as the analysis relied only on one sample. Maximal root depth was relatively similar for all treatments and the majority of the roots was systematically contained in the upper 15–20 cm (from 82.8 to 98.7% of the total root biomass given the treatment). In Fig. 3(b), T66low seems to induce a higher root concentration in the upper 10 cm (77.3% of root biomass contained in the 0–10 cm layer, 21.3% in the 10–20 cm layer), while T66high possesses a more constant root density until a depth of 20 cm (40.8% from 0 to 10 cm; 42.0% from 10 to 20 cm). This behavior suggests an adaptation of the root development to the irrigation schedule when the plant is subject to water stress. Root adaptation to the zone of high soil moisture for various plant species was also observed by Gorla et al. (2015), Zotarelli et al. (2009) and Phene et al. (1991).

3.3. Model calibration and validation

After calculation of the soil and meteorological parameters, calibration of the root water uptake reduction function was critical, as it directly influences water stress. Calibration of the parameters of that function (h_{50} and p) was done using the data from experiment T66high from 80 to 95 DAT. Using the same climatic input and field data and the root zone distribution measured in the field, different values were tested. The RMSE between observed and modeled SMP at 5, 10 and 15 cm was then calculated over the whole simulation period and was compared with other statistical parameters such as the Coefficient of determination (R^2), the slope from the linear model, the Modeling efficiency (EF) and the Coefficient of Residual Mass (CRM). The three best sets of parameters were h_{50} =−40 kPa, p = 3; h_{50} =−50 kPa, p = 3 and h_{50} =−50 kPa, p = 4. The second set of parameters was selected as it best simulated the decrease in SMP just before an irrigation event (Fig. 4), which was essential to correctly calibrate the root water uptake reduction function. The calibration with the selected parameters was then tested with different values of the water stress index ω_c which is used for water uptake compensation. A value between 0.6 and 0.8 led to the lowest RMSE. A value of 0.7 was selected for further simulations to allow an early transpiration reduction and a high sensitivity to water stress.

Due to irregularities in the water distribution of the drip system and inhomogeneities in the soil texture, a perfect fit between the modeled and measured SMP was not possible. Moreover, the root distribution used in the model was time independent which does not allow any growth or modification during the simulation.

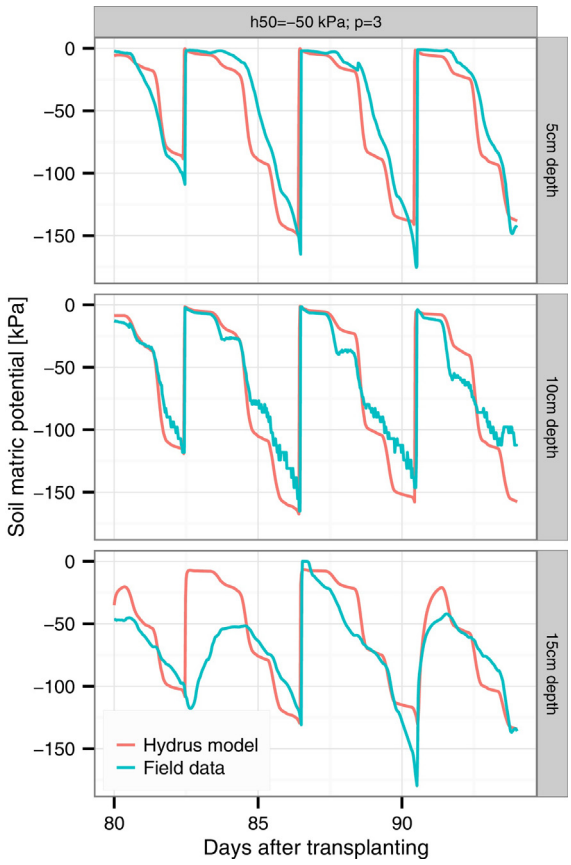

Fig. 4. Comparison between modeled and measured SMP for T66low at 5, 10 and 15 cm depth from 80 to 94 DAT for the best set of parameters.

The parameters of the selected root water uptake reduction function were validated by comparing simulated and observed SMP from the other experiments. In particular, it was verified that the minimum SMP values before the irrigation events were similar. For instance, for T100high, for the same simulation period, using the best set of parameters, the RMSE over time were 25.7 kPa and 23.4 kPa at 5 and 15 cm respectively and the RMSE before the irrigation events were 17.9 kPa and 11.8 kPa at 5 and 15 cm respectively.

Interestingly, for all treatments, it was found that the simulated water front after an irrigation event only reached a depth of 20–25 cm. This could also be observed from the SMP measurements, where the sensors at 15 cm depth partially reacted to the irrigation events (Fig. 1). From the root density analysis, the root structure did not seem to have been greatly affected by the rocky layer, as only few finer roots reached this depth and were not packed just above it. It seems that the roots developed primarily in the upper 25 cm where water was most available. The depth of the root zone and wetted front was therefore mainly linked to the different irrigation schedules. For this reason, for the hypothetical scenarios, the maximal root depth and the maximal horizontal length of the roots were defined to match the dimension of the wetted bulb simulated by the model.

Finally, the calculated ratio of actual over maximal transpiration (T_a/T_{max}) for the four treatments from 80 to 95 DAT were the following: T150low: 99.9%; T66low: 76.4%; T100high: 84.1% and T66high: 65.3%. These ratios seem to accurately reflect the magnitude of water stress when compared to the measured crop yield in Table 5. It was concluded that transpiration reduction from HYDRUS 2D/3D can be used as a good indicator of water stress for further simulations.

3.4. Impact of the irrigation threshold and irrigation depth

Different simulations were built for the early growth stage and the mid-season stage by varying the irrigation thresholds and the irrigation depth. Fig. 5 shows the calculated ratio of transpiration reduction (T_a/T_{max}) and the ratio of irrigation water applied to the crop (Irr) to the crop maximal evapotranspiration (ETc_{max}) for all scenarios. ETc_{max} was calculated based on Kc_{max} in the dual crop coefficient as described in Allen et al. (1998) and assumes maximal soil evaporation ($K_r = 1$). Colored ribbons were drawn to show the optimal threshold region given the irrigation depth. Two parameters were used: First, the higher value of the ribbon was selected to avoid unnecessary water losses from evaporation and leakages. It was located just after the sharp drop of the $irrigation/ET_c$ ratio and the start of a flatter zone in Fig. 5(b) and (d). Secondly, the lower ribbon value corresponded to the onset of transpiration reduction (lower than 99% of maximal transpiration) to avoid water stress in Fig. 5(a) and (c).

3.4.1. Early growth stage

Fig. 5(a) and (b) shows the results for the early growth stage. The irrigation threshold decreases with increasing irrigation depths at 5 cm, due to a more complete recharge of the root zone soil moisture, and the optimal threshold values correspond to −15 kPa, −25 kPa and −35 kPa for an irrigation depth of 1.4, 2.8 and 5.6 mm respectively. The irrigation water needs corresponding to those thresholds are the same, around 42% of ETc_{max}. With higher thresholds, too frequent irrigations lead to a higher soil evaporation, while beyond these thresholds, the irrigation amounts decrease more slowly, as most of the water losses are minimized, so that only transpiration reduction reduces the irrigation water needs.

Due to the low irrigation depths, the threshold could only have been placed at 5 cm depth. Based on the simulations with a threshold at 5 cm depth, the corresponding minimum SMP value at other depths can be numerically monitored. Fig. 6 shows the evolution of the SMP for the three selected scenarios. With an irrigation depth of 1.4 and 2.8 mm, the corresponding SMP at 10 cm depth decreases up to −20 kPa. However, due to the low irrigation depth, the SMP is not always completely recharged and falls below −20 kPa. For the irrigation depth of 5.6 mm, the SMP at 10 cm decreases up to −15 kPa. Below 10 cm depth, the SMP hardly fluctuates with time due to low root water uptake.

For the early growth stage, a sensor depth of 5 cm is adequate but the optimal threshold depends on the irrigation depth. At 5 cm depth, a threshold of −15 to −20 kPa is recommended in order to avoid water stress even for low irrigation depths (Fig. 5(a)), while keeping water losses relatively low even with higher irrigation depths (Fig. 5(b)). A maximal sensor depth of 10 cm can also be recommended since even low irrigation depths can be monitored, but not below. At 10 cm depth, the threshold has a smaller optimal range between −15 and −20 kPa to avoid water stress, though this could not be validated by direct simulations.

3.4.2. Mid-season stage

Fig. 5(c) and (d) shows the results for the mid-season. It appears that the beginning of transpiration reduction occurs at relatively similar thresholds, around −40 kPa for 11.3 mm and −50 kPa for 22.6 mm. Additionally, it seems that a threshold of −30 kPa would be sufficient to avoid most water losses regardless of the irrigation depth. It is therefore recommended to use a threshold value between −30 and −40 kPa to trigger irrigation at 10 cm depth, which avoids most water losses while maintaining maximal transpiration.

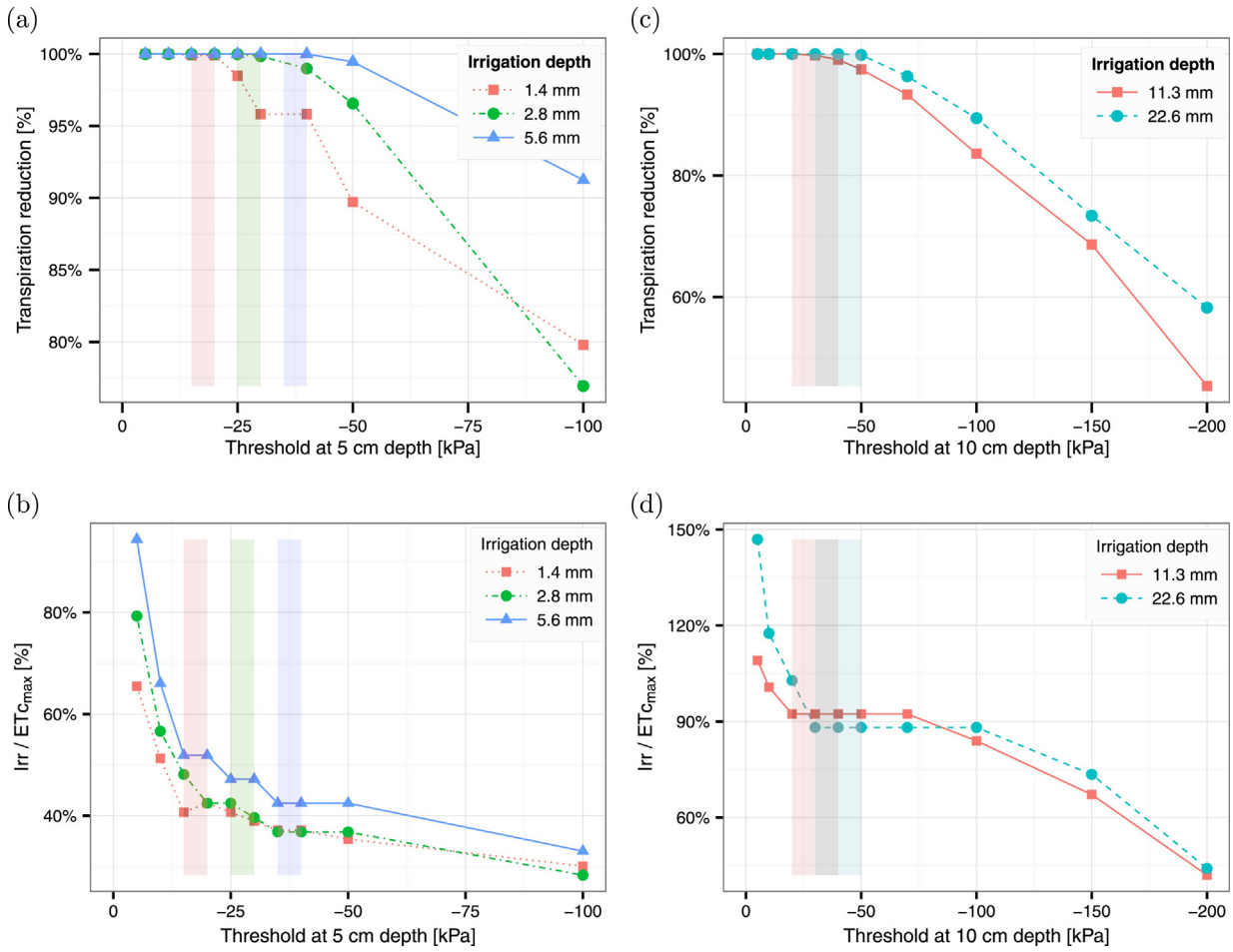

Fig. 5. Results of all scenarios for varying irrigation thresholds at 5 cm depth for the early growth stage and 10 cm depth for the mid-season and for different irrigation depth. (a) and (b) represent scenarios for the early growth stage (10–30 DAT); (c) and (d) show the results for the mid-season (60–80 DAT); (a) and (c) show the simulated cumulative actual transpiration volumes over the cumulative maximal transpiration amounts. (b) and (d) represent the reduction in irrigation water applied to the crop, using the ratio of cumulative irrigation amounts (*Irr*) to the cumulative amounts of maximal crop evapotranspiration (ETc_{max}). The colored ribbons show the regions of optimal thresholds given the irrigation depth (higher value avoids water losses, lower value limits transpiration reduction). (For interpretation of the references to color in this figure legend, the reader is referred to the web version of the article.)

3.5. Impact of the soil texture

For the mid-season stage, the influence of different soil textures on the optimality of the selected thresholds was also evaluated. Indeed, texture influences the SMP and root distribution, so that it may impact on the threshold, given the sensor depth. Similarly to Fig. 5, scenarios were built by varying the irrigation threshold and testing different soil types with a single irrigation depth of 11.3 mm. Textures from coarse soils (sandy loam) to fine textures (silt, clay loam) were used based on the parametrization of Carsel

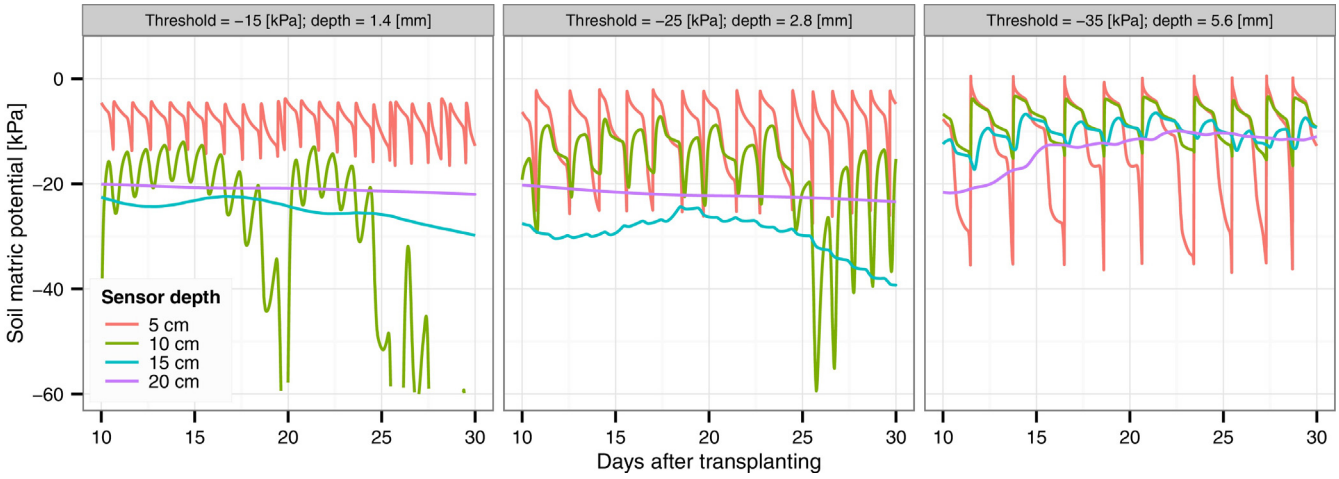

Fig. 6. Evolution of the SMP at different sensor depths with time for the three optimal scenarios of the early growth stage with a threshold at 5 cm depth.

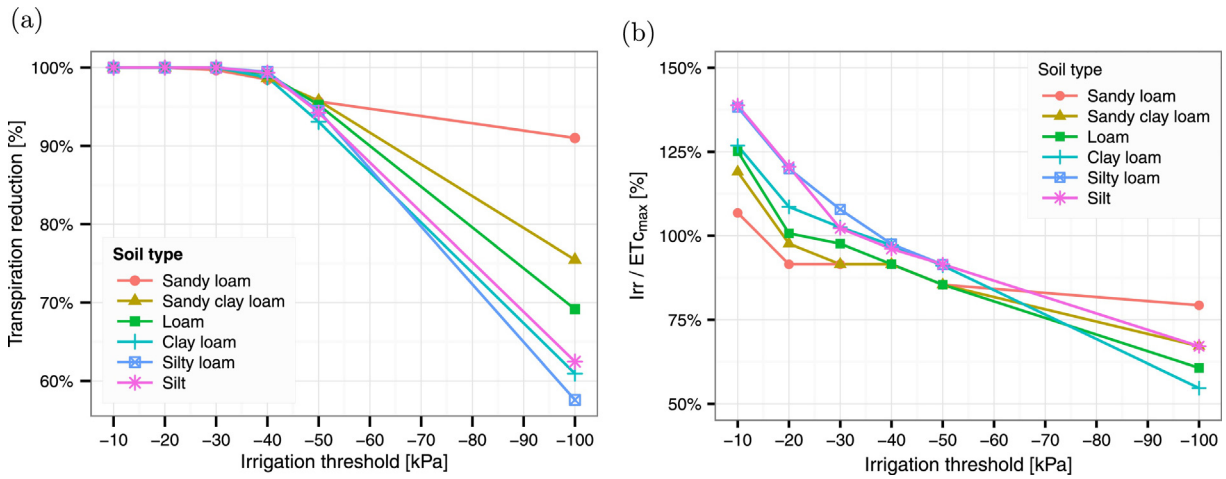

Fig. 7. (a) Ratio of actual over maximal transpiration; (b) ratio of cumulative irrigation amounts (*Irr*) over cumulative maximal crop evapotranspiration (ETc_{max}) for the mid-season, and for different soil textures.

and Parrish (1988). Fig. 7 shows the results. The threshold emerges clearly for all soils at −40 kPa, as there is hardly any transpiration reduction. Using a threshold at −30 kPa seems less adequate, since irrigation amounts are still relatively high for the finer soil textures. It appears that by placing the sensor near the depth where maximal root water uptake takes place, it is possible to define a stable threshold independently of the soil texture.

4. Discussion

Two complementary approaches were used in this study to acquire a complete understanding of the complex relationship between soil water dynamics and plant response. The numerical model enabled us to consider the SMP at multiple locations given the depth and the horizontal distance from the dripper, and not only at a single point measurement, as it is the case with a sensor. This allows a better analysis of the spatial evolution of the SMP and the corresponding root water uptake response. In parallel, the field measurements were used to calibrate and validate the model and the water stress function.

4.1. Crop response to water stress

Field experiments show that T150low, the control treatment, led to optimal fruit yield and was the only experiment which did not suffer from water stress. The SMP was kept mostly between 0 and −15 kPa but the soil was not completely saturated so that no significant soil aeration problems seem to have occurred. The constantly wetter soil surface led however to higher water losses which led to a lower IWUE for T150low (Table 5). During the crop development stage (20-60 DAT), the high irrigation depth with a low frequency (every 2 days) applied for T100high led to water stress and suboptimal aerial biomass development. In contrast, restoring only 66% of ET_c with a lower irrigation depth and a higher frequency did not influence the plant growth of T66low. Referring to the SMP evolution (Fig. 1), it seems preferable to irrigate regularly and to maintain the SMP above −50 kPa in the top 10 cm (T66low) rather than to apply a lower irrigation frequency, letting the SMP drop below −50 kPa at both 5 and 15 cm depth (T100high).

During the mid-season (60–100 DAT), when root depth becomes maximum, the high depth and low frequency of T100high was better tolerated as the plants' biomass catches up with the level of T150low and T66low and the final yields of T66low and T100high were similar. It is likely that yield was limited mainly because of reduced biomass development for T100high during the development stage, while fruit development was limited during the mid-season for T66low due to the partial provision of the water needs. It therefore seems that a SMP threshold higher than −50 kPa at 5 cm depth only results in optimal yields when a higher irrigation depth recharges the soil at least in the top 15 cm. Below −100 kPa at both 5 and 15 cm depth, fruit development was considerably reduced (T66high). As a general conclusion, eggplants seem to tolerate a decrease in SMP of up to −50 kPa if the whole root zone is recharged by the irrigation events.

4.2. Threshold sensitivity

The threshold selected from the different models is clearly dependent on the transpiration reduction function, and the water stress index (ω_c) which allow water uptake compensation.

In order to assess the sensitivity of the threshold, additional simulations were performed with a more sensitive transpiration reduction function with h_{50} =−30 kPa. Results show that transpiration reduction occurs earlier, with a decrease of 3.5% with a threshold of −30 kPa and of 8.8% with a threshold of −40 kPa. It appears therefore that, even with a very sensitive reduction function that is exaggerated for eggplants, transpiration is kept relatively high, so that the threshold of −40 kPa appears quite robust.

The effect of the water stress index (ω_c) on the transpiration reduction was also evaluated by running our best selected scenario (threshold of −40 kPa at 10 cm depth, with an irrigation depth of 11.3 mm) with different values of ω_c. Table 6 shows the ratio of actual over potential transpiration given different values of ω_c.

Compensation clearly influences transpiration reduction. A value of ω_c of 1 or even 0.9 however does not seem realistic with our model. Indeed, in the model, the root water uptake is directly linked to the spatial root distribution without compensation (Šimůnek and Hopmans, 2009), so that it cannot evolve spatially in time and does not adapt to the water availability in the soil. The compensation could therefore be seen as a dynamic adaptation of the root zone to the soil moisture. Such rapid root water uptake adaptation was discussed by Coelho and Or (1998) as resulting from rapid growth of fine roots or changes in root conductivity. A ω_c value

Table 6
Ratio of actual over potential transpiration (T_a / T_p) given different values of ω_c for a threshold of −40 kPa at 10 cm depth and an irrigation depth of 11.3 mm.

ω_c	0.5	0.6	0.7	0.8	0.9	1
T_a/T_p	1	0.998	0.991	0.973	0.921	0.906

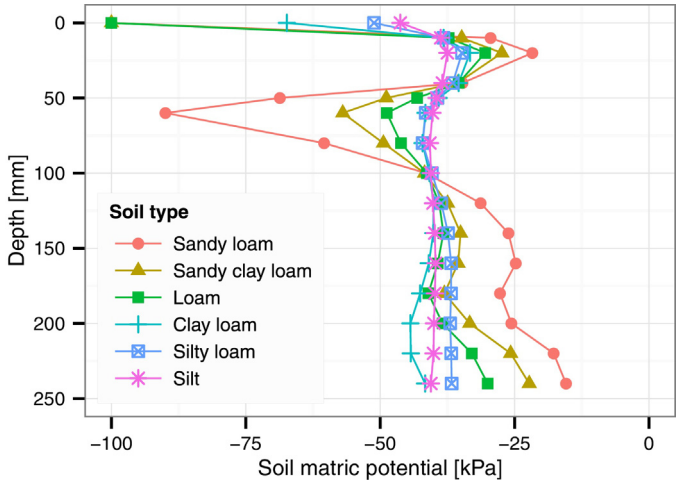

Fig. 8. SMP distribution with depth just before an irrigation event for a threshold of −40 kPa at 10 cm depth.

of 0.7 represents a low adaptivity of the root water uptake, and is likely underestimated. The threshold of −40 kPa is consequently sensitive to water stress.

4.3. SMP distribution and impact on the sensor location

The numerical simulations showed that the root zone SMP cannot be considered to be homogeneous. Fig. 8 shows the SMP distribution with depth just before an irrigation event for an irrigation threshold of −40 kPa at 10 cm depth and different soil textures. It appears that the SMP distribution is dependent on the soil texture. Indeed, the coarser textures show greater SMP variations in depth than for finer soils (clay loam, silty loam, silt).

For instance, if the sensor were placed at 20 cm depth, the threshold would be −35 kPa for a silty loam texture and only −25 kPa for a sandy soil. This is mainly due to the relationship between soil moisture and SMP. In the case of sandy loam, most of the soil moisture has been depleted below −20 kPa, so that further water uptake leads to a rapid decrease in SMP. Additionally, coarse soils have lower unsaturated hydraulic conductivity. For sandy loam, a SMP drop started occurring just a few hours before the irrigation event, where root density was maximal at a depth of 70 mm. This illustrates that water stress occurs differently given the soil texture. In coarse soils, stress occurs more rapidly and severely in a specific zone of the root system, while in finer soils, a milder but longer stress occurs in the whole root system.

In coarse soils, the sensor location is therefore essential: it should be placed in the zone of maximal root density in order to monitor the onset of water stress. If the sensor is placed below this zone, the threshold must be set higher in order to avoid possible stress in the upper part of the root zone. In finer soil textures, the SMP appears more homogeneous so that the sensor location is less important in monitoring the onset of water stress. Placing the sensor near the zone of maximal water uptake is recommended in order to measure a representative value of water stress.

4.4. Recommended sensor position

From the field experiments and numerical simulations, it is recommended to place the sensor at a depth of 10 cm and at a horizontal distance of 5 cm from the dripper. It is assumed here that the dripper is located near the plant stem. There are different reasons for this optimal location. From the results at the early growth stage, the best sensor depth is located between 5 and 10 cm depth. Below 10 cm depth, almost no variations in SMP occur so that a lower depth is inadequate to control irrigation (Fig. 6). This is validated by the field measurements, where each sensor at 15 cm depth hardly responded to the irrigation events at 20 to 40 DAT (Fig. 1). During the mid-season, 10 cm depth appeared to be an adequate sensor depth as it matched the depth of maximal root density and water uptake. Using a shallow sensor depth such as 5 cm may however not be optimal. Indeed, if the irrigation depth is low, only the top soil will be wetted and water stress at lower root depth will not be monitored. This was observed from the field experiment T66low in Fig. 1 where the SMP remained mostly above −40 kPa at 5 cm depth while the SMP decreased below −200 kPa at 15 cm and led to limited crop yield.

Based on the goal to manage irrigation during the whole crop growth with a single sensor at a fixed depth, we conclude that using a sensor depth of 10 cm will provide the most efficient irrigation system. Indeed, this depth seems to be the best trade-off between early and mid-season stages. During the very early stage, this recommendation should be used carefully, as 10 cm was not directly verified by numerical simulations and root length may depend on the seedling age.

10 cm depth is therefore recommended for plants with shallow root systems. Considering semi-arid regions, this placement is deemed adequate as most soils are compact and usually shallow (Dembele and Some, 1991).

Regarding the horizontal placement of the sensor, a maximal distance of 5 cm away from the plant stem was adequate. At greater distance, little fluctuations in SMP were observed during the early growth stage. During the mid-season, this distance showed clear fluctuations in SMP and better response to the irrigation events so that it was considered adequate. Finally, Dabach et al. (2015) also showed that placing the sensor closer than 10 cm from the dripper leads to more stable measurements given variations in the spatial soil structure, and they recommend placing the sensor near the dripper.

Finally, in this study, we only propose an optimal sensor location and threshold to optimize irrigation, but we do not consider variations in the soil structure over the crop or differences in root water uptake or transpiration rates between plants. The number of sensors needed to acquire a representative measurement of the whole crop state is not discussed and goes beyond the scope of this study.

Table 7
Summary of the procedure to determine the irrigation threshold given the plant growth stage. The different growth stages are based on the classification used by the FAO in Allen et al. (1998).

Crop stage	Threshold (10 cm depth)
10 DAT to end of the initial growth	−15 kPa
Crop development	Linear decrease from −15 kPa to −40 kPa
Mid-season	−40 kPa

4.5. Recommended thresholds

Table 7 summarizes the recommended thresholds for the whole growing period at 10 cm depth. The period of establishment between sowing and transplanting is not taken into account.

The first ten days after transplantation are critical, since roots may still be shallow. It is recommended to irrigate every day during ten days and then to start using thresholds. At the early growth stage, results converged towards a threshold of −15 kPa at 10 cm depth, though 5 cm sensor depth was also adequate. During the crop development stage, root development and deepening mainly increase the zone of root water uptake. Assuming the same sensitivity to water stress (same transpiration reduction function), we propose lowering the threshold from −15 kPa to −40 kPa linearly

with time, reflecting the growth of the root system. Marouelli and Silva (2007) reported that the crop development period is less sensitive to water stress for tomatoes, which is in the same family as eggplants, so that even lower thresholds may be found adequate. In the mid-season, a threshold of −40 kPa at 10 cm depth allowed the most water savings while keeping maximal transpiration and was adequate for different soil textures.

Thresholds were found adequate for a wide range of the irrigation depth at 10 cm. However, using a very low irrigation depth will result in a smaller wetted area and root zone, which may lead to a lower capacity to uptake essential nutrients. Nutrients uptake was not part of our simulations but should be considered in further studies. On the contrary, if more than 150% of the RAW is used, leakages will occur which will not be monitored by our single sensor system. A moderate irrigation depth of around 75% of the RAW can be recommended.

Simulations showed that most water savings can be achieved at the early growth stage in comparison with the maximal crop evapotranspiration (ETc_{max}). This is due to the much higher soil evaporation rate during that stage. On the other hand, during the mid-season, the optimal irrigation needs are located at around 90% of ETc_{max}. This is in agreement with the FAO directives and the results of Lovelli et al. (2007) who showed that providing 100% of ET_c for eggplant growth was indeed the most profitable irrigation schedule.

The crop root distribution may also influence the adequacy of the threshold at 10 cm depth, since a different root density pattern will modify the soil water dynamics. However, literature has shown that most vegetable crops (tomato, cucumber, watermelon, squash, onion, etc.) have the majority of their roots in the upper 30 cm (Weaver and Bruner, 1927; Zotarelli et al., 2009). Moreover, our experiments, as well as Coelho and Or (1998), showed that the root structure adapts its density to the location where water availability is optimized, which will be around the sensor depth in the case of drip irrigation.

In the context of semi-arid regions, it seems that the recommended system may perform well in different semi-arid regions. Indeed, climatic conditions are characterized by a high evaporative rate and most soils are sandy and dense. Concerning different crops, field experiments should be run to assess their specific tolerance to water stress. However, it seems possible that the thresholds proposed in this study may be applied to other vegetable crops, as the selected transpiration reduction function was relatively sensitive to water stress, and as the root distribution of most vegetable crops is likely to be concentrated in the top 30 cm.

5. Conclusion

The combination of field experiments and numerical models allowed for a better understanding of the complex interactions between water stress, root water uptake, soil water dynamics and thresholds definition. While the field experiments allowed us to assess biomass and yield production in comparison with some local SMP measurements, the model allowed a more generalized appreciation of the root zone soil water dynamics as a whole. Numerical simulations using HYDRUS 2D/3D appeared to be a powerful tool to generalize site-specific experiments. The study therefore emphasized the importance of taking into account the soil water dynamics when relating a single SMP measurement to water stress in order to propose reproducible irrigation thresholds. In particular, numerical results showed the great impact of the root distribution on the soil water dynamics and the importance of the sensor location to define thresholds. For a better understanding of the onset and the dynamics of water stress, more research is needed to link the spatial distribution of soil water availability with root architecture and to characterize the linked effects on root water uptake, compensation and reallocation. Results also emphasized the great potential of water savings before the mid-season, a period during which few thresholds have been recommended. Remarkably, it was shown that irrigating using a single SMP sensor at 10 cm depth with evolving thresholds during crop growth was appropriate to provide an eggplant, and possibly other vegetable plants, with an optimal input of water to optimize yields while limiting most water losses independently of the soil texture. In contrast to most site-specific researches, those reference thresholds were designed for practical use by local producers in semi-arid regions.

Acknowledgments

This study is part of the project Info4Dourou2.0 managed by the Cooperation & Development Center (CODEV) based at the Ecole Polytechnique Fédérale de Lausanne (EPFL) which aims to improve water management by the use of simple low-cost wireless sensor networks. We thank the team of engineers in Burkina Faso who offered an essential support to the experiments. We warmly thank the nonprofit social enterprise *International Development Enterprises* (iDE) in Burkina Faso for the provision of their crops and technical support for the duration of our experiments. We also thank the *Sensorscope* company that manufactured the wireless sensor network and offered their technical support. PP wishes to thank the Swiss National Science Foundation for financial support through the grant REMEDY (PP00P2-153028/1).

References

Allen, R.G., Pereira, L.S., Raes Dirk, Martin, S., 1998. Crop evapotranspiration – Guidelines for computing crop water requirements – FAO Irrigation and drainage paper 56. Rome. http://www.kimberly.uidaho.edu/water/fao56/fao56.pdf.

Anon, 2003. Analyse des résultats de l'enquête maraichère camapgne 1996 à 1997. Technical Report. Ministère de l'agriculture de l'hydraulique et des ressources halieutiques, Secrétariat général, Direction générale des prévisions et des statistiques agricoles. Direction des statistiques agricoles, Ouagadougou.

Barrenetxea, G., Ingelrest, F., Schaefer, G., Vetterli, M.,2008. The Hitchhiker's guide to successful wireless sensor network deployments. In: Proceedings of the 6th ACM conference on Embedded network sensor systems – SenSys '08. ACM Press, New York, NY, USA, pp. 43–56, http://dx.doi.org/10.1145/1460412.1460418.

Bilibio, C., Carvalho, J.a., Martins, M., Rezende, F.C., Freitas, E.a., Gomes, L.a.a., 2010. Vegetative growth and yield of eggplant under different soil water tensions. Rev. Brasil. Eng. Agríc. Ambient. 14, 730–735, http://dx.doi.org/10.1590/S1415-43662010000700007.

Carsel, R.F., Parrish, R.S., 1988. Developing joint probability distributions of soil water retention characteristics. Water Resour. Res. 24, 755–769, http://dx.doi.org/10.1029/WR024i005p00755.

Coelho, E.F., Or, D., 1998. Root distribution and water uptake patterns of corn under surface and subsurface drip irrigation. Plant Soil 206, 123–136, http://dx.doi.org/10.1023/A:1004325219804.

Coolong, T., Snyder, J., Warner, R., Strang, J., Surendran, S., 2012. The relationship between soil water potential, environmental factors, and plant moisture status for poblano pepper grown using tensiometer-scheduled irrigation. Int. J. Veg. Sci. 18, 137–152, http://dx.doi.org/10.1080/19315260.2011.591483.

Coolong, T., Surendran, S., Warner, R., 2011. Evaluation of irrigation threshold and duration for tomato grown in a silt loam soil. HortTechnology 21, 466–473 http://horttech.ashspublications.org/content/21/4/466.short.

Dabach, S., Lazarovitch, N., Šimunek, J., Shani, U., 2013. Numerical investigation of irrigation scheduling based on soil water status. Irrig. Sci. 31, 27–36, http://dx.doi.org/10.1007/s00271-011-0289-x.

Dabach, S., Shani, U., Lazarovitch, N., 2015. Optimal tensiometer placement for high-frequency subsurface drip irrigation management in heterogeneous soils. Agric. Water Manage. 152, 91–98, http://dx.doi.org/10.1016/j.agwat.2015.01.003.

Deb, S.K., Shukla, M.K., Mexal, J.G., 2011. Numerical modeling of water fluxes in the root zone of a mature pecan orchard. Soil Sci. Soc. Am. J. 75, 1667–1680, http://dx.doi.org/10.2136/sssaj2011.0086.

Dembele, Y., Some, L., 1991. Propriétés Hydrodynamiques des Principaux Types de sol du Burkina Faso. INERA, Ouagadougou.

Enciso, J., Wiedenfeld, B., Jifon, J., Nelson, S., 2009. Onion yield and quality response to two irrigation scheduling strategies. Sci. Hortic. 120, 301–305, http://dx.doi.org/10.1016/j.scienta.2008.11.004.

FAO, 2014. Climate-Smart Agriculture Sourcebook. Food and Agriculture Organization of the United Nations, Rome http://www.fao.org/docrep/018/i3325e/i3325e00.htm.
FAO, 2014. Innovation in Family Farming. Number 2014 in The State of Food and Agriculture. Food and Agriculture Organization of the United Nations, Rome http://www.fao.org/publications/sofa/2014/en/.
Fondio, L., N'Tamon, L., Hala, F., Dijdji, H., 2009. Evaluation agronomique de six cultivars d'aubergine africaine (Solanum spp.) de la nouvelle collection des plantes légumières du CNRA. Agron. Afr. 20, 69–79, http://dx.doi.org/10.4314/aga.v20i1.1737.
van Genuchten, M.T., 1980. A closed-form equation for predicting the hydraulic conductivity of unsaturated soils. Soil Sci. Soc. Am. J. 44, 892–898, http://dx.doi.org/10.2136/sssaj1980.03615995004400050002x.
van Genuchten, M.T., 1987. A numerical model for water and solute movement in and below the root zone. Research Report No 121. U.S. Salinity Laboratory, USDA, ARS, Riverside, CA https://books.google.ch/books?id=sPe5YgEACAAJ.
Gorla, L., Signarbieux, C., Turberg, P., Buttler, A., Perona, P., 2015. Transient response of Salix cuttings to changing water level regimes. Water Resour. Res. 51, 1758–1774, http://dx.doi.org/10.1002/2014WR015543 arXiv:2014WR016527.
Kang, Y., Wan, S., 2005. Effect of soil water potential on radish (*Raphanus sativus* L.) growth and water use under drip irrigation. Sci. Hortic. 106, 275–292, http://dx.doi.org/10.1016/j.scienta.2005.03.012.
Laio, F., Porporato, A., Fernandez-Illescas, C., Rodriguez-Iturbe, I., 2001. Plants in water-controlled ecosystems: active role in hydrologic processes and response to water stress. Adv. Water Resour. 24, 745–762, http://dx.doi.org/10.1016/S0309-1708(01)00007-0.
Liu, H., Yang, H., Zheng, J., Jia, D., Wang, J., Li, Y., Huang, G., 2012. Irrigation scheduling strategies based on soil matric potential on yield and fruit quality of mulched-drip irrigated chili pepper in Northwest China. Agric. Water Manage. 115, 232–241, http://dx.doi.org/10.1016/j.agwat.2012.09.009.
Lovelli, S., Perniola, M., Ferrara, A., Di Tommaso, T., 2007. Yield response factor to water (Ky) and water use efficiency of *Carthamus tinctorius* L. and *Solanum melongena* L. Agric. Water Manage. 92, 73–80, http://dx.doi.org/10.1016/j.agwat.2007.05.005.
Marouelli, W.A., Silva, W.L.C., 2007. Water tension thresholds for processing tomatoes under drip irrigation in Central Brazil. Irrig. Sci. 25, 411–418, http://dx.doi.org/10.1007/s00271-006-0056-6.
Mermoud, a., Tamini, T., Yacouba, H., 2005. Impacts of different irrigation schedules on the water balance components of an onion crop in a semi-arid zone. Agric. Water Manage. 77, 282–295, http://dx.doi.org/10.1016/j.agwat.2004.09.033.
Oliveira, E.C., Carvalho, J.D.a., Silva, W.G.D., Rezende, F.C., Almeida, W.F.D., 2011. Effects of water deficit in two phenological stages on production of Japanese cucumber cultived in greenhouse. Eng. Agríc. 31, 676–686, http://dx.doi.org/10.1590/S0100-69162011000400006.
Pasquale, N., Perona, P., Francis, R., Burlando, P., 2012. Effects of streamflow variability on the vertical root density distribution of willow cutting experiments. Ecol. Eng. 40, 167–172, http://dx.doi.org/10.1016/j.ecoleng.2011.12.002.
Patakas, A., Noitsakis, B., Chouzouri, A., 2005. Optimization of irrigation water use in grapevines using the relationship between transpiration and plant water status. Agric. Ecosyst. Environ. 106, 253–259, http://dx.doi.org/10.1016/j.agee.2004.10.013.
Phene, C., Davis, K., Hutmacher, R., Bar-Yosef, B., Meek, D., Misaki, J., 1991. Effect of high frequency surface and subsurface drip irrigation on root distribution of sweet corn. Irrig. Sci. 12, 135–140, http://dx.doi.org/10.1007/BF00192284.
Raes, D., Steduto, P., Hsiao, T.C., Fereres, E., 2012. Chapter 3: Calculation procedures. In: Aquacrop Reference Manual verion 4.0 – Reference Manual. FAO – Food and Agriculture Organization of the United Nations, Rome, pp. 125.
Ranquet Bouleau, C., Baracchini, T., Barrenetxea, G., Repetti, A., Bolay, J.C., 2015. Low-cost wireless sensor networks for dryland irrigation agriculture in Burkina Faso. In: Technologies for Development. Springer International Publishing, pp. 19–31, http://dx.doi.org/10.1007/978-3-319-16247-8_3.
Steduto, P., Hsiao, T.C., Fereres, E., Raes, D., 2012. Crop Yield Response to Water – FAO Irrigation and Drainage Paper No.66. Rome. http://www.fao.org/docrep/016/i2800e/i2800e00.htm.
Šimůnek, J., van Genuchten, M.T., Šejna, M., 2012. The HYDRUS Software Package for Simulating the Two- and Three-Dimensional Movement of Water, Heat, and Multiple Solutes in Variably-Saturated Porous Media Technical, Technical Manual, Version 2.0. PC-Progress, Prague, Czech Republic.
Šimůnek, J., Hopmans, J.W., 2009. Modeling compensated root water and nutrient uptake. Ecol. Model. 220, 505–521, http://dx.doi.org/10.1016/j.ecolmodel.2008.11.004.
Taghvaeian, S., Chávez, J., Hansen, N., 2012. Infrared thermometry to estimate crop water stress index and water use of irrigated maize in Northeastern Colorado. Remote Sens. 4, 3619–3637, http://dx.doi.org/10.3390/rs4113619.
Thompson, R., Gallardo, M., Valdez, L., Fernández, M., 2007. Using plant water status to define threshold values for irrigation management of vegetable crops using soil moisture sensors. Agric. Water Manage. 88, 147–158, http://dx.doi.org/10.1016/j.agwat.2006.10.007.
Wang, D., Kang, Y., Wan, S., 2007a. Effect of soil matric potential on tomato yield and water use under drip irrigation condition. Agric. Water Manage. 87, 180–186, http://dx.doi.org/10.1016/j.agwat.2006.06.021.
Wang, F.X., Kang, Y., Liu, S.P., Hou, X.Y., 2007b. Effects of soil matric potential on potato growth under drip irrigation in the North China Plain. Agric. Water Manage. 88, 34–42, http://dx.doi.org/10.1016/j.agwat.2006.08.006.
Wang, Q., Klassen, W., Li, Y., Codallo, M., Abdul-Baki, A.a., 2005. Influence of cover crops and irrigation rates on tomato yields and quality in a subtropical region. HortScience 40, 2125–2131 http://handle.nal.usda.gov/10113/19049.
Weaver, J.E., Bruner, W.E., 1927. Root Development of Vegetable Crops. McGraw-Hill Book Company, Incorporated https://sustainablefarmer.com/pdflibrary/library-rootdevelopment.pdf.
Yadav, B.K., Mathur, S., Siebel, M.A., 2009. Soil moisture dynamics modeling considering the root compensation mechanism for water uptake by plants. J. Hydrol. Eng. 14, 913–922, http://dx.doi.org/10.1061/(ASCE)HE.1943-5584.0000066.
Zheng, J., Huang, G., Jia, D., Wang, J., Mota, M., Pereira, L.S., Huang, Q., Xu, X., Liu, H., 2013. Responses of drip irrigated tomato (*Solanum lycopersicum* L.) yield, quality and water productivity to various soil matric potential thresholds in an arid region of Northwest China. Agric. Water Manage. 129, 181–193, http://dx.doi.org/10.1016/j.agwat.2013.08.001.
Zotarelli, L., Scholberg, J.M., Dukes, M.D., Muñoz-Carpena, R., Icerman, J., 2009. Tomato yield, biomass accumulation, root distribution and irrigation water use efficiency on a sandy soil, as affected by nitrogen rate and irrigation scheduling. Agric. Water Manage. 96, 23–34, http://dx.doi.org/10.1016/j.agwat.2008.06.007.